European Review for Medical and Pharmacological Sciences 2023; 27: 3681-3698

Exploration at the network pharmacology level of possible targeting mechanisms of Smilacis Glabrae Rhixoma for the treatment of osteoporosis

B.-W. LU[1], X.-Z. LIANG[2,3], M.-T. WEN[2], G. LI[2,3]

[1]College of Traditional Chinese Medicine, Shandong University of Traditional Chinese Medicine, Shandong, China
[2]First College of Clinical Medicine, Shandong University of Traditional Chinese Medicine, Shandong, China
[3]Orthopaedic Microsurgery, Affiliated Hospital of Shandong University of Traditional Chinese Medicine, Shandong, China

Abstract. – OBJECTIVE: The aim of this study was to evaluate the therapeutic effect of Smilacis Glabrae Rhixoma (SGR) on osteoporosis at the level of network pharmacology, and to find new targets and mechanisms of SGR in the treatment of osteoporosis, to better find new drugs and their clinical applications.

MATERIALS AND METHODS: In the original network pharmacology mode, we used an improved mode, such as screening the ingredients and targets of SGR through tools such as GEO database, Autodock Vina, and GROMACS. Through molecular docking, we conducted further screening for the targets acting on the effective ingredients of SGR, and finally we performed molecular dynamics simulation and consulted a large amount of related literature for the validation of the results.

RESULTS: By screening and validating the data, we finally confirmed that there were mainly 10 active ingredients in SGR, which were isoeruboside b, smilagenin, diosgenin, stigmasterol, beta-sitosterol, sodium taurocholate, sitogluside, 4,7-dihydroxy-5-methoxy-6-methyl-8-formyl-flavan, simiglaside B, and simiglaside E, and mainly acted on eleven targets. These targets mainly exert therapeutic effects on osteoporosis by regulating 20 signaling pathways including Th17 cell differentiation, HIF-1 signaling pathway, apoptosis, inflammatory bowel disease, and osteoclast differentiation.

CONCLUSIONS: Our study successfully explains the effective mechanism by which SGR ameliorates osteoporosis while predicting the potential targets NFKB1 and CTSK of SGR for the treatment of osteoporosis, which provides a novel basis for investigating the mechanism of action of new Traditional Chinese medicines (TCMs) at the network pharmacology level and a great support for subsequent studies on osteoporosis.

Key Words:
Osteoporosis, Smilacis Glabrae Rhixoma, Molecular dynamics, CTSK, ADMET.

Abbreviations

Smilacis Glabrae Rhixoma (SGR); Traditional Chinese medicine (TCM); oral bioavailability (OB); drug similarity (DL); Biological Process (BP); Cellular Component (CC); Fold Change (FC); Gene Expression Omnibus (GEO); Gene Ontology (GO); Kyoto Encyclopedia of Genes and Genomes (KEGG); Molecular Function (MF); National Center for Biotechnology Information (NCBI); Protein-Protein Interaction (PPI); Bisphosphonates (BPs).

Introduction

Osteoporosis is one of the most common bone diseases in clinics. It is an age-related disease with decreased bone mass, destruction of bone tissue microstructure, increased bone fragility, and fracture prone[1]. Zeng et al[2] recruited 75,321 Chinese adults aged 20 and above to systematically measure bone mineral density (BMD) values in 10 years and found that the prevalence of osteoporosis in Chinese men and women aged 50 and above was 6.46% and 29.13%. It is estimated that by 2035, the number of fractures related to osteoporosis will reach 4.83 million every year, and the annual cost will be about 19.92 billion US dollars[3]. Modern medical treatment of osteoporosis is mainly hormone and calcitonin drugs,

Corresponding Author: G. Li, MD; e-mail: sdszylg@163.com

which cost more and have greater side effects. The effect of traditional Chinese medicine in treating osteoporosis is significant, and the price is low, and the side effects are small. Osteoporosis belongs to the traditional Chinese medicine "bone withered", "bone impotence", "bone erosion", and other categories. In the syndrome differentiation of traditional Chinese medicine, kidney essence deficiency syndrome is the most common.

Traditional Chinese medicine (TCM) is a disease treatment method originated in China. It is completely different from the treatment of Western medicine. The components of TCM are mixed. A traditional Chinese medicine often has many components, which can act on many disease targets. It is the multi-component and multi-target function that makes traditional Chinese medicine particularly important in the treatment of difficult and complex diseases. *Smilacis Glabrae Rhixoma* (SGR) is the dry rhizome of *Smilax glabra*, a *Liliaceae* plant. It is mainly distributed in provinces south of the Yangtze River, such as Hubei, Hunan, Zhejiang, Yunnan, Guangdong, and other places. It has the effects of detoxification, dehumidification, and joint benefit. There has always been a saying in Chinese folk that SGR can treat osteoporosis. However, there is no relevant literature to report the effect and mechanism of SGR in treating osteoporosis. Therefore, it is important to immediately reveal the molecular mechanism of SGR in treating osteoporosis.

In this study, we broke the traditional animal models, cell migration and other methods, and used the recently popular method of effective components and target mining of traditional Chinese Medicine-Network pharmacology. Network pharmacology is a new research method in recent years, which was first proposed by Hopkins, a professor of pharmacology at Dundee University in the UK. This method is based on the theory of system biology, which is a new subject that selects specific signal nodes for multi-target drug molecular design. In order to improve the therapeutic effect of drugs and reduce their toxic and side effects, so as to improve the success rate of clinical trials of new drugs and save the cost of drug research and development, network pharmacology emphasizes the multi-channel regulation of target on signal pathway. Therefore, we will analyze and study the components and target mechanisms of SGR in the treatment and prevention of osteoporosis through network pharmacological methods, combined with gene expression analysis, molecular docking, and molecular dynamics simulation.

Materials and Methods

Screening the Active Ingredients of SGR

TCMSP database of Traditional Chinese Medicine System Pharmacology database and analysis platform[4] is one of the most commonly used databases for screening active ingredients of Traditional Chinese medicine. Its advantage is that the database gives oral bioavailability (OB) and drug similarity (DL) parameters, which play an essential role in the evaluation of drug efficacy. Only when these two values exceed a certain value (OB $\geq$ 25% and DL > 0 or OB > 0% and DL $\geq$ 0.18), can effectively reflect the generic properties of a component.

Among them, the calculation of the DL value of the system follows formula (1). In order to obtain the target drug, the DL value will work only when the lead compound is chemically easy to be synthesized and has the properties of ADMET (absorption, distribution, metabolism, excretion and toxicity)[5].

(1)
$$T(x,y) = \frac{\mathrm{x-y}}{|x|^2+|y|^2-xy}$$

X in formula (1) represents the descriptive index of all components in SGR, and Y represents the average drug similarity index of this component from DrugBank database[6].

The lipid water partition coefficient refers to the partition coefficient of drugs in the n-octanol-water system, which is widely used as a measure of the hydrophobicity of chemical components. It represents the main driving force of effective components through the biofilm composed of lipid bilayers, which controls the combination of components and targets. is one of the expression methods of . Generally, the range of the required value is -0.4 to 5.6. The calculation of follows formula (2):

(2)
$$logP_{\frac{o}{w}} = \frac{\log C_O}{\log C_W}$$

In formula (2), CO represents the equilibrium concentration of the drug in the oil phase, and CW represents the equilibrium concentration of the drug in the water phase. The value of indicates the hydrophobicity of the solute. The greater the , the stronger the hydrophobicity. On the contrary, the stronger the hydrophilicity.

Get the Targets of SGR and Osteoporosis

In order to study the mechanism of the targeted treatment of osteoporosis with active ingredients of SGR, first of all, we must obtain the targets that all active ingredients can act on. Secondly, we need to obtain the targets of osteoporosis that have been verified clinically. Only by finding the common parts of these two kinds of targets, can we continue to study this experiment.

We searched the above obtained SGR active components in TCMSP database, obtained all the targets corresponding to SGR chemical components, merged them with the osteoporosis targets we obtained in the DisGeNET database[7], and then took Venn to coincide, to obtain the final required disease target information.

Construction of PPI and H-C-T-D Network

In order to clearly show the corresponding relationship between SGR and its active components, targets and osteoporosis, we used Cytoscape 3.8.0 software[8] (available at: https://cytoscape.org/download.html) to visually construct the H-C-T-D network for the above active components and targets and obtain the H-C-T-D network diagram we needed. In this network diagram, we used different node shapes and colors to represent each content. So far, we have completed the preliminary screening of the osteoporosis related active ingredients of SGR.

In order to obtain the disease targets with interaction relationship, we performed protein interaction analysis (PPI analysis) on all preliminarily screened targets. We presented the enrichment p-value < 1.0e-16 as the analysis condition. After PPI network analysis, we obtained the action relationship network of all proteins. According to this network diagram, we obtained the further screened osteoporosis targets.

GEO Gene Expression Analysis

The difference between the geo database from National Center for Biotechnology Information (NCBI) and The Cancer Genome Atlas (TCGA) database is that the GEO database not only contains cancer-related clinical information, but also has many non-cancer clinical information, which makes the GEO database perfect in providing clinical case information.

In order to further screen the active ingredients, we have preliminarily screened the target of their action, we obtained enough clinical case samples of osteoporosis (including 10 clinical samples) from the GSE35956 dataset (GPL570 platform) of GEO database. Through the gene expression analysis of GSE clinical samples, we drew an intuitive gene expression heat map to screen the target again.

Gene Enrichment Analysis and Construction of C-T-P Network

To assess the interaction between the targets screened above, protein interaction networks and active component-target-pathway network (C-T-P networks) were constructed. To explore the biological processes and pathways that each target participates in *in vivo*, data of target genes were retrieved through DAVID Bioinformatics Resources[9]. Bioprocess (BP) analysis with GO (Gene Ontology) analysis and KEGG (Kyoto Encyclopedia of Genes and Genomes) enrichment analysis were performed. The false discovery rate (FDR) of GO analysis and KEGG enrichment analysis all meet the requirements of significant gene enrichment *in vivo* and have statistical significance (FDR < 0.05).

The FDR value is a p-value that should be corrected and used to screen out results that are more accurate. Therefore, this step is intended to obtain biological processes and *in vivo* pathways for target action, providing a basis for future research.

ADMET Prediction of Effective Components in SGR

Absorption (A), distribution (D), metabolism (M), excretion (E), and toxicity (T) of drugs have always been an important part of all drug studies. As a result, there are many tools for predicting ADMET. Although the accuracy of these tools is uneven, there is still a widely recognized tool, ADMETlab 2.0 (available at: https://admetmesh.scbdd.com). ADMETlab 2.0[10] is a well-known and accurate ADMET prediction tool. Here, we use ADMETlab 2.0 to predict the ADMET values of active compounds for future researchers to refer to these data.

Molecular Docking

Molecular docking is a method of drug design through the interaction between receptors and drug molecules. It is a theoretical simulation method that studies interactions between molecules, such as ligands and receptors, and predicts their binding modes and affinity. In recent years, molecular docking has become an important technology in the field of computer-aided drug research[11].

The effective components of SGR are docked to the precise molecules of the osteoporosis tar-

get with tools such as AutoDock Vina software[12] (available at: https://vina.scripps.edu) and PyMol software[13] (available at: https://pymol.org/2/). The binding energy of the components to the target is used to verify the reliability of the effective components of SGR in the treatment of osteoporosis, and further exclude the components of SGR that are less effective in the treatment of osteoporosis.

Validation of Gromacs Molecular Dynamics Simulation

On the basis of molecular docking and GSE gene difference analysis, we carried out molecular dynamics simulation (MD simulation) to validate the results. MD simulation is a method that simulates the movement of small molecules in the body environment by a computer. We used Gromacs software[14] (available at: https://www.gromacs.org) to simulate MD, set the physical conditions as constant temperature (310K), constant pressure (101kPa), and periodic boundary conditions, and used TIP3P water model. The human environment was simulated in 0.145 mol/L neutral sodium chloride solution. After the state balance of all environments was carried out, we used the selected component-target complex system to perform 50 ns of MD simulation, in which the conformation was stored every 10 ps. The root mean square deviation (RMSD) and radius of gyration (Rg) analysis and visualization of MD simulation results were performed using Gromacs embedded program and VMD, and we know that, Rg of protein reflects the volume and structure state of protein macromolecules. The larger the Rg value of the same system, the larger the expansion of the system occurs during the process of MD, and the stability of the system is poor.

Results

Screening Results of SGR Active Components

Thirty-five known active ingredients from SGR were collected from TCMSP database, including lipids, flavonoids, flavonoids, amino acids, etc. Under two screening conditions: OB > 25% and DL > 0, FASA (value < 0.339) or OB > 0% and DL > 0.18, FASA (< 0.339), and 13 effective pharmaceutical components were selected from 35 SGR compounds. The screening details of these 13 components are shown in Table I. Among them, MW is the relative molecular weight of compounds, OB represents the oral bioavailability of compounds, Hdon and Hacc represent the hydrogen donor and hydrogen acceptor of compounds, DL is drug-likeness, and FASA is the fractional water accessible surface area. All values have been verified by TCMSP database and are accurate and effective.

Acquisition of Coincident Targets and Construction Results of PPI Network

After screening, we obtained 1,729 targets of 13 SGR active ingredients through SuperPred database (338 after removing duplicate values). At the same time, we obtained 1,098 and 4,657 osteoporosis targets using the DisGeNET database and Genecards database, respectively. Then, by taking the coincidence of SGR and osteoporosis targets, we obtained the Venn diagram of the number of overlapping targets between SGR and osteoporosis (Figure 1). In the Venn diagram, we showed that there were 72 overlapping targets between SGR and osteoporosis.

In order to obtain disease targets with interaction relationship, we analyzed the PPI network of 72 preliminarily screened targets. We found that there was no interaction between alox12, gpr35, HPSE and other targets, so we abandoned them. Using string database and Cytoscape, we constructed the PPI network of the remaining 69 targets (Figure 2), which contains 465 edges, the darker the color of the line, the stronger the interaction of these targets (p-value < 1.0e-16), that is, these targets are more likely to become candidate targets for osteoporosis. Therefore, we obtained the osteoporosis target after further screening.

It is clear that in Figure 2, there are many targets that interact most strongly with each other, such as MYC (Myc proto-oncogene protein), STAT3 (Signal transducer and activator of transcription 3), HSP90AA1 (Heat shock protein HSP 90-alpha), HIF1A (Hypoxia-inducible factor 1 alpha), ESR1 (Estrogen receptor alpha), MTOR (Serine/threonine-protein mTOR), TLR4 (Toll-like receptor 4), PIK3CA (PI3-kinase p110-alpha subunit), *CXCR4* (C-X-C chemokine receptor type 4), MAPK1 (MAP kinase ERK2), MAPK1 (MAP kinase ERK2), MAPK14 (MAP kinase p38 alpha), MMP2 (Matrix metalloproteinase-2), PTPN11 (Protein-tyrosine phosphatase 2C), STAT1 (Signal transducer and activator of transcription 1-alpha/beta), CXCR4 (C-X-C-C chemokine receptor receptor type 4), MAPK1 (MAP kinase ERK2), MAPK14 (MAP kinase p38 alpha alpha), MMP2P2P2P2P2P2P2P2 (Matrix metalloprotro-

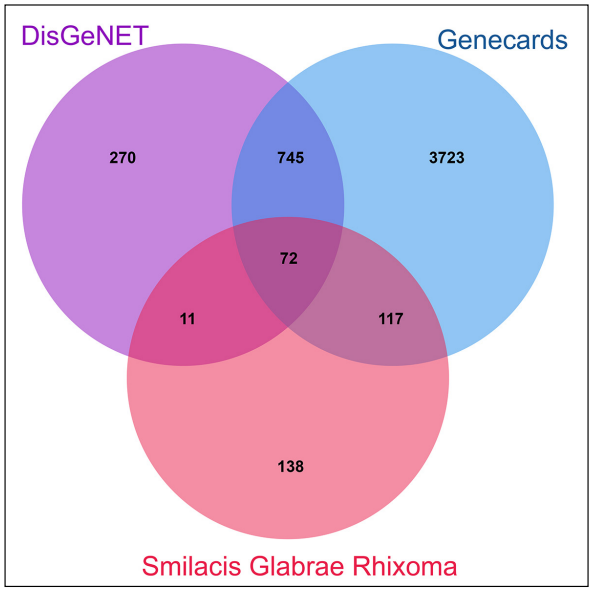

Figure 1. Intersection of SGR target and osteoporosis target.

troteinase-oxide synthase, endothelial). Although some proteins clearly may not interact with other proteins, they may also play an important role in osteoporosis symptoms.

Results of H-C-T-D Network Construction and GSE Gene Expression Analysis

To make a one-to-one correspondence between the 13 active components of SGR and its 69 intersecting targets of osteoporosis, we constructed a H-C-T-D network using Cytoscape software (Figure 3). From the H-C-T-D network, we found that the 13 components of SGR ranked as strong or weak components of target are Sodium taurocholate, isobaimuxinol, isoeruboside B, stigmasterol, smilagenin, diosgenin, beta-sitosterol, sitogide, simiglaside E, respectively. simiglaside D, simiglaside B, simiglaside C, and 4,7-Dihydroxy-5-methoxyl-6-methyl-8-formyl-flavan. The darker the color of a target, the more likely it is to be a candidate target for osteoporosis.

To ensure the accuracy of the experimental data, we further screened the components and targets. Through the GEO database, we obtained 20,549 osteoporosis-related disease genes from the GSE35956 dataset. It is undeniable that these osteoporosis gene expression data have high reference values. These genes correspond to 10 osteoporosis clinical infection samples from the GSE35956 dataset. From these 10 osteoporosis case samples, we selected the expression data of 69 genes that we needed, and then used R 4.0.2 (available at: https://www.r-project.org) visual programming language to draw a thermal map of gene differences (Figure 4).

Based on gene diversity analysis of GSE clinical samples, we excluded 55 targets with no significant differences among the remaining 69 targets, and 14 osteoporosis targets with differentially expressed levels ranging from high to low were HIF1A, HSP90AA1, CTSB, SERPINE1, GSTP1, APEX1, STAT1, HDAC1, LMNA, CTSK, TGM2, STAT3, NFKB1 and DPP4. Among them, the expression levels of HIF1A, HSP90AA1, CTSB, and

Table I. Screening information of 14 compounds in SGR.

Molecular name	MW	OB	Alogp	Hdon	Hacc	DL	FASA	PubChem CID
Sitogluside	576.95	20.63194	6.337	4	6	0.6241	0.227022	5742590
beta-sitosterol	414.79	36.91391	8.084	1	1	0.75123	0.225506	222284
Stigmasterol	412.77	43.82985	7.64	1	1	0.75665	0.216794	5280794
diosgenin	414.69	80.87792	4.634	1	3	0.80979	0.190773	99474
Smilagenin	416.71	14.15272	4.884	1	3	0.80715	0.193609	91439
Isobaimuxinol	238.41	98.37846	2.448	1	2	0.14231	0.19723	128735
4,7-Dihydroxy-5-methoxyl-6-methyl-8-formyl-flavan	314.36	37.03309	2.693	2	5	0.27872	0.301456	129394
Simiglaside B	954.96	3.038519	3.13	6	22	0.19682	0.309495	11658052
Simiglaside C	820.82	4.214839	1.282	5	20	0.30901	0.273838	11972467
Simiglaside D	966.97	3.047874	3.525	5	22	0.19225	0.319887	102369777
Simiglaside E	924.93	3.165505	3.146	6	21	0.21612	0.327553	11764506
Sodium taurocholate	514.78	15.19777	1.193	4	8	0.86358	0.053834	23666345
Isoeruboside B	432.71	13.34044	3.715	2	4	0.79012	0.220859	194485

Molecular weight (MW), oral bioavailability (OB), hydrogen donor (Hdon), hydrogen acceptor (Hacc), drug-likeness (DL), fractional water accessible surface area (FASA).

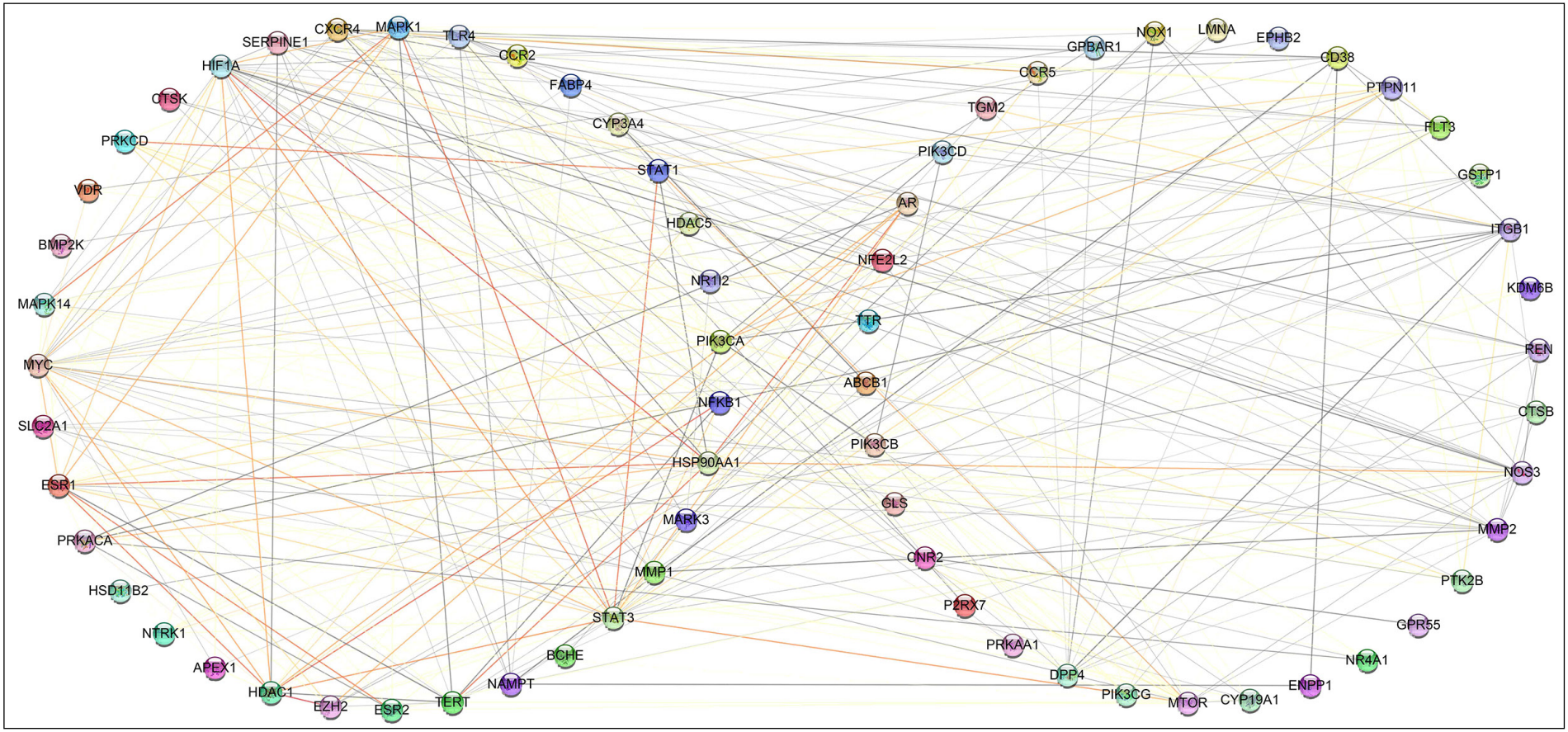

Figure 2. PPI network with 69 targets.

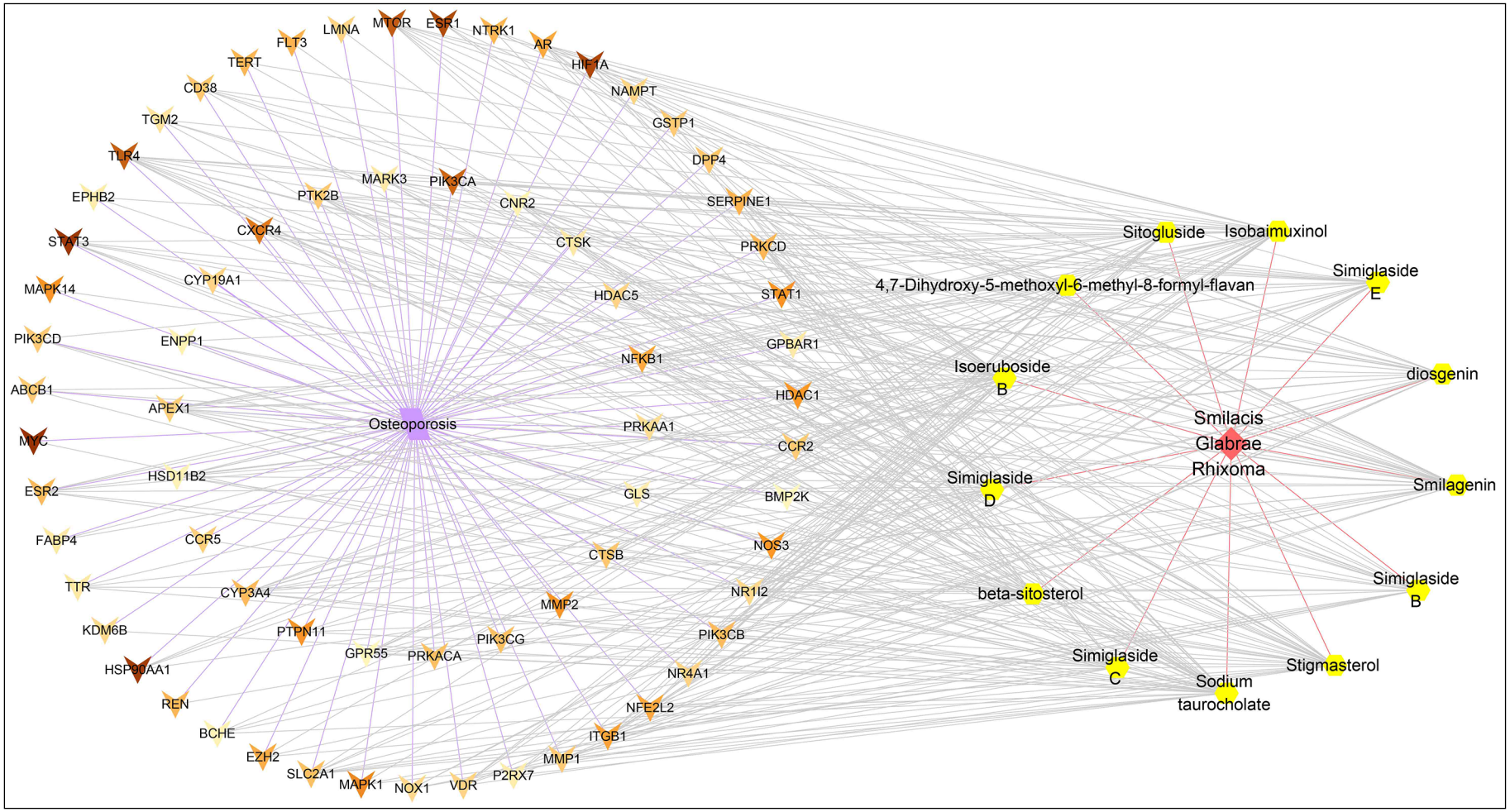

Figure 3. Six components of SGR and H-C-T-D network of osteoporosis targets.

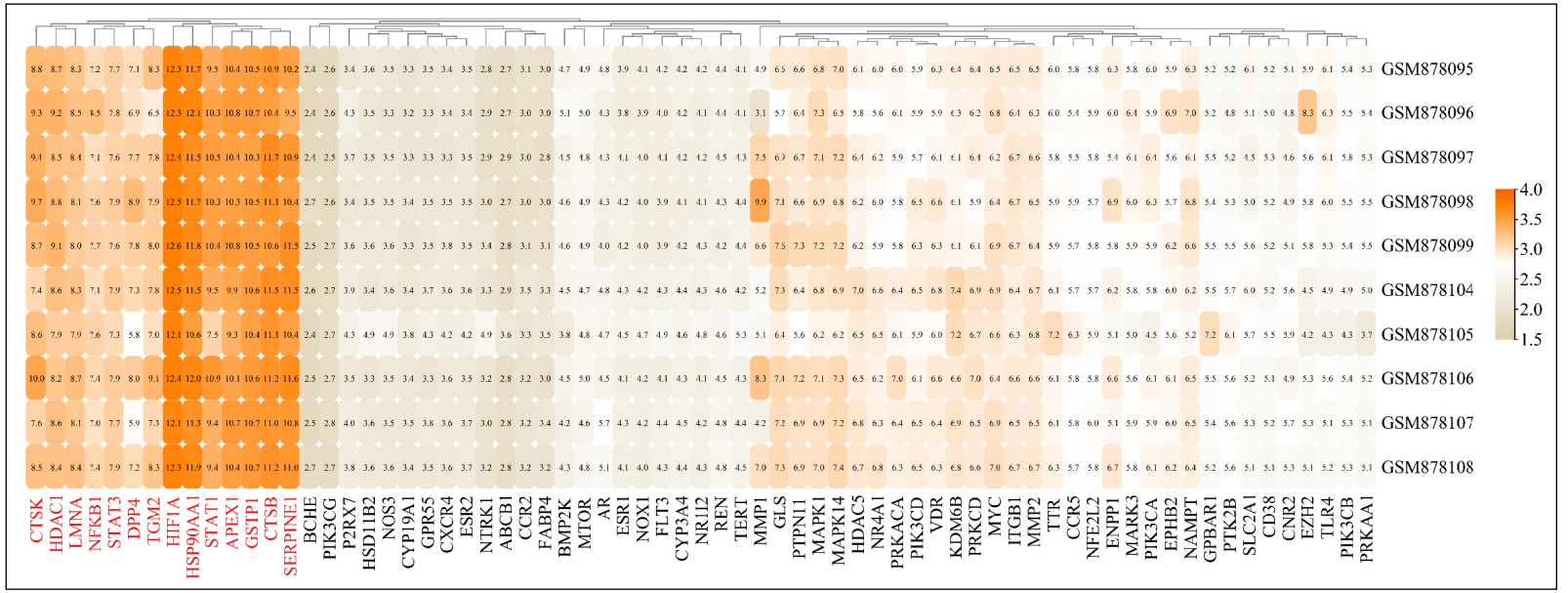

Figure 4. Thermogram of gene differentiation for 28 targets.

SERPINE1 in osteoporosis patients were significantly higher than other targets.

Enrichment Analysis

Based on gene expression analysis of GSE clinical samples, we obtained 14 osteoporosis high expression targets, which were HIF1A, HSP90AA1, CTSB, SERPINE1, GSTP1, APEX1, STAT1, HDAC1, LMNA, CTSK, TGM2, STAT3, NFKB1 and DPP4. The results showed that both male osteoporosis[15] and female postmenopausal osteoporosis[16] had high expression of HIF1A. The same is true for the remaining targets, so we performed GO enrichment analysis on the remaining 14 targets and plotted a column graph (Figure 5) representing the three GO entries.

To ensure the reliability and statistical significance of the data, we used 14 targets in the DAVID database to perform KEGG enrichment analysis with p-value < 0.005. Three of the 20 pathways, TGM2, DPP4, and APEX1, did not exist, so we discarded them, and then we presented 20 pathways in a thermal graph from the results we considered together (Figure 6).

We analyzed 20 KEGG pathways and found that KEGG pathways revealed most of the pathways related to osteoclast differentiation, cancer, diabetes, inflammation, etc. In osteoporosis, these pathways are mainly enriched in Th17 cell differentiation, HIF-1 signaling pathway, apoptosis, inflammatory bowel disease, and osteoclast differentiation. In the discussion section, we will specifically describe the role of target regulatory pathways.

Analysis of C-T-P Network Construction Results

Referring to the results of KEGG enrichment analysis, we linked 13 components, 11 targets and 20 pathways to construct an H-C-T-P network diagram (Figure 7) to visualize the relationships between components and targets, and between targets and pathways. A total of 44 nodes and 129 edges of C-T-P network were obtained.

From the C-T-P network, according to the number of component targeting proteins, we first sorted 12 active components of SGR: Isoeruboside B, Sodium taurocholate, Isobaimuxinol, Smilagenin, beta-sitosterol, 4,7-Dihydroxy-5-methoxyl-6-methyl-8-formyl-fla, Simiglaside B, Simiglaside C, Simiglaside D, Simiglaside E, Stiigerol, diosgmin, and Sitogluside. According to the number of target regulatory pathways, we ranked 11 osteoporosis targets as NFKB1, STAT1, STAT3, HIF1A, HSP90AA1, CTSK, GSTP1, HDAC1, CTSB, SERPINE1, and LMNA. Then a portion of the 20 pathways were ranked according to the number of target points of regulatory pathways, as Pathin cancer, Th17 cell differentiation, HIF-1 signaling pathway, apoptosis, NOD-like receptor signaling pathway, AGE-RAGE signaling pathway complications in betcations, Kaposi sarcoma-associated herpesvirus infection, Epstein-Barr virus infection, programmed cell death ligand 1 (PD-L1) expression and programmed death-1 (PD-1) checkpoint pathway in cancer, necroptosis, and osteoclast differentiation. However, although these targets and pathways may contribute to the development of osteoporosis, the accuracy of these contributions remains indistinguishable, and further analysis and validation are required.

Results of ADMET Prediction

In the predicted results of ADMET (Table II), 13 candidate compounds for treatment from SGR are listed. The information in the table includes five indicators of ADMET, of which human colorectal adenocarcinoma cell permeability (Caco-2 Permeability) and human intestinal absorption (HIA) are included in absorption. When the value of Caco-2 Permeability is greater than -5.15 log unit, compound performance is defined as excellent, and the closer the HIA value is to 1, the better the compound is absorbed in the human intestine. Distribution contains blood-brain barrier penetration (BBB Penetration), which works better when the value of BBB Penetration is closer to 1. Metabolism includes three indicators of hepatic drug enzyme subfamily inhibitors, CYP2C19, CYP2C9, and CYP2D6. Similarly, when they are closer to 1, they are more likely to become inhibitors. In the excretion section, two indicators, clearance (CL) and half-life ($T_{1/2}$), are defined as high clearance when CL is greater than 15 mL/min/kg, medium clearance when CL is 5-15 mL/min/kg, and short half-life when $T_{1/2}$ is lower than 3.

The most important part of ADMET is toxicity. In this part, we provide four toxicity indices for 13 compounds: human ether-a-go-go blockers (hERG Blockers), human hepatotoxicity (H-HT), drug induced liver injury (DILI), and respiratory toxicity. The higher these values, the more toxic they will be.

Analysis of Molecular Docking Results 18

Table II. ADMET predictions for 13 compounds.

	Absorption		Distribution	Metabolism (inhibitor)			Excretion		Toxicity			
PubChem CID	HIA	Caco-2 Permeability	BBB Penetration	CYP2C19	CYP2C9	CYP2D6	CL	T1/2	hERG Blockers	H-HT	DILI	Respiratory Toxicity
5742590	0.01	-4.793	0.01	0.024	0.124	0.014	3.083	0.131	0.891	0.163	0.179	0.89
222284	0.002	-4.679	0.136	0.143	0.208	0.142	7.21	0.049	0.875	0.131	0.551	0.464
5280794	0.009	-4.576	0.178	0.17	0.346	0.295	4.515	0.036	0.31	0.188	0.237	0.807
99474	0.003	-4.706	0.447	0.132	0.239	0.053	13.253	0.074	0.982	0.365	0.602	0.982
91439	0.003	-4.799	0.155	0.103	0.246	0.023	16.237	0.132	0.996	0.29	0.828	0.956
128735	0.003	-4.576	0.256	0.05	0.089	0.02	11.261	0.23	0.035	0.832	0.034	0.946
129394	0.007	-4.937	0.749	0.356	0.356	0.016	4.995	0.195	0.025	0.041	0.139	0.548
11658052	0.995	-6.037	0.028	0.233	0.793	0.361	5.442	0.965	0.215	0.61	0.434	0.018
11972467	0.995	-6.076	0.088	0.076	0.221	0.11	3.606	0.961	0.237	0.878	0.887	0.023
102369777	0.995	-5.87	0.031	0.333	0.724	0.485	3.504	0.958	0.225	0.746	0.849	0.019
11764506	0.995	-6.098	0.032	0.295	0.766	0.391	3.909	0.958	0.226	0.215	0.235	0.013
23666345	0.353	-5.148	0.72	0.004	0.024	0	4.563	0.212	0.04	0.347	0.015	0.302
194485	1	-6.379	0.163	0	0	0	0.234	0.044	0.039	0.17	0.02	0.008

Colorectal adenocarcinoma cell permeability (Caco-2 Permeability), human intestinal absorption (HIA), blood-brain barrier penetration (BBB Penetration), clearance (CL), half-life (T1/2), human ether-a-go-go blockers (hERG Blockers), human hepatotoxicity (H-HT), Drug Induced Liver Injury (DILI).

After a series of analysis, screening and validation work, we have identified the target sites of 13 SGR components acting on each other. After obtaining this information, we used Chemdraw 19.0 software[17] (available at: https://perkinelmerinformatics.com/products/research/chemdraw) to draw the structure of six components, save them as mol2 files, use PDB database[18] to select the corresponding protein tertiary structure with ligands based on the structure of the components and download the PDB file. The PDB protein files were processed by PyMol software (removal of water molecules and redundant structures, etc.), two file formats were saved as pdbqt files using AutoDock software, ligands and coordinate locations (x, y, z) were selected, and the components were sorted and sorted by the distance of hydrogen bonds. These tertiary structures were predicted by X-ray diffraction or solution NMR methods. Then, we used AutoDock and AutoDock Vina to dock the components to the target molecule. The docking results are shown in Table III. We sorted the docking results and selected 14 pairs of component-target complexes with better results to visualize their results using PyMol (Figure 8).

To ensure data availability and reference value, we set the coordinates (x, y, z) according to the structure size of the component itself. It is known that the larger the value of the coordinate, the greater the affinity for docking; the greater the affinity, proving that the closer the component binds to the target, the more effective the component is. Therefore, these coordinate values are most appropriate for the component itself. The docking results showed that the binding energy (kcal/mol) of the components to the target was -8.7 kcal/mol and -4.7 kcal/mol. From the visualization results, we can see that the effective components of the eight SGRs, diosgenin, stigmasterol, smilagenin, isoeruboside B, beta-sitosterol, sodium taurocholate, sitogluside and similaglaside B, all bind well to the corresponding target, and the hydrogen bond distance is stable within 3.5.

Analysis of MD Simulation Results

RMSD and Rg values are important criteria to measure the stability of the complex system of components and proteins, the stability of the tertiary structure of proteins combined with small molecules, and the hydrophobicity of amino acid residues. Therefore, we selected five targets and one of their corresponding components for MD simulation. In order to make these data more intuitive to our eyes, we visualized their output data (Figure 9).

Based on the results of the RMSD simulation, it can be seen that the blue polyline, HDAC1-Smilagenin, does not perform well in the five MD systems of the component and target complex, including the large fluctuation of RMSD and the large Rg value, which means that the system does not exhibit effective inhibition against osteoporosis.

Four other MD systems (NFKB1-Diosgenin, CTSK-Stigmasterol, CTSB-Stigmasterol, and LMNA-Taurocholic acid) exhibit very stable fluctuations in RMSD and Rg values. Therefore, we can conclude that the three components of SGR, diosgenin, stigmasterol, and taurocholic acid, can stably target the four targets of NFKB1, CTSK, CTSB, and LMNA, and can play a good role in the treatment of osteoporosis. However, this result does not mean that other targets (STAT3, SERPINE1, GSTP1, and HSP90AA1, etc.) are not important in the treatment of osteoporosis. Instead, their importance awaits more research and exploration.

Discussion

Osteoporosis is mainly due to osteoclast's greater bone resorption than osteoblast's bone remodeling, resulting in loss of bone mass, and in a series of symptoms such as bone fragility, fracture, and pain. Osteoclasts are the major functional cells for bone resorption and play an important role in bone development, growth, repair, and reconstruction. Osteoclast, originating from the monocyte-macrophage system, is a special terminal differentiation cell that can be fused by its monocyte precursor cells in various ways to form large multinucleated cells. Bisphosphonates (BPs) are a new class of drugs used in various bone diseases and calcium metabolic diseases. It binds specifically to hydroxyphosphate in bones and inhibits osteoclast activity, thereby inhibiting bone resorption. However, long-term administration of BPs has been reported[19,20] to cause femoral fractures, and intravenous administration of BPs or Denosumab causes necrosis of articular bone. Cathepsin K (CTSK) is a lysosomal cysteine protease and the major cathepsin expressed in osteoclasts. It can degrade bone matrix. Therefore, CTSK is a potential therapeutic target for osteoporosis. Researchers[21,22] suggest that CTSK inhibitors may be used to block bone resorption. Therefore, it is necessary to find a new type of CTSK inhibitor to prevent bone

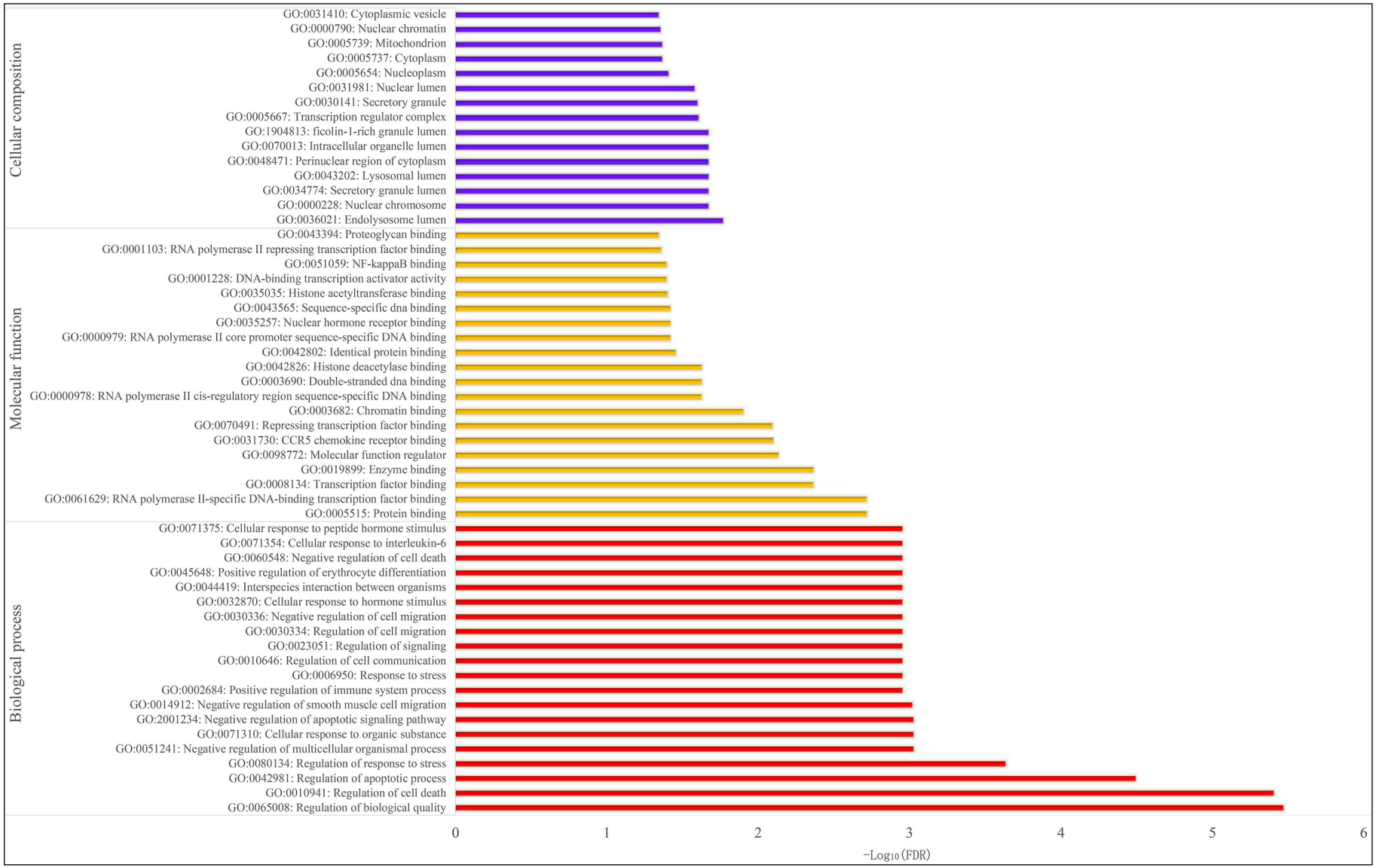

Figure 5. GO enrichment analysis of the screened 14 targets.

Table III. Docking results of 13 active components of SGR and target molecules of osteoporosis..

PubChem CID	Compounds	Targets	Affinity (kcal/mol)	UniProt ID	PDB ID	Role of original ligand
194485	Isoeruboside B	STAT3	-8.7	P40763	6NJS	Inhibitor
91439	Smilagenin	STAT3	-8.5	P40763	6NJS	Inhibitor
99474	diosgenin	NFKB1	-8.4	P19838	2O61	Inhibitor
99474	diosgenin	STAT3	-8.3	P40763	6NJS	Inhibitor
194485	Isoeruboside B	SERPINE1	-8.2	P05121	7AQF	Inhibitor
91439	Smilagenin	HSP90AA1	-8.1	P07900	5J80	Inhibitor
99474	diosgenin	SERPINE1	-8.1	P05121	7AQF	Inhibitor
5280794	Stigmasterol	CTSK	-8	P43235	4X6H	Inhibitor
91439	Smilagenin	HDAC1	-7.9	Q13547	4BKX	Inhibitor
91439	Smilagenin	NFKB1	-7.9	P19838	2O61	Inhibitor
91439	Smilagenin	SERPINE1	-7.9	P05121	7AQF	Inhibitor
5280794	Stigmasterol	CTSB	-7.6	P07858	6AY2	Inhibitor
222284	beta-sitosterol	GSTP1	-7.6	P09211	5J41	Inhibitor
194485	Isoeruboside B	NFKB1	-7.6	P19838	2O61	Inhibitor
5280794	Stigmasterol	STAT3	-7.6	P40763	6NJS	Inhibitor
222284	beta-sitosterol	CTSK	-7.5	P43235	4X6H	Inhibitor
23666345	Sodium taurocholate	CTSB	-7.4	P07858	6AY2	Inhibitor
23666345	Sodium taurocholate	HDAC1	-7.3	Q13547	4BKX	Inhibitor
5742590	Sitogluside	CTSB	-7.2	P07858	6AY2	Inhibitor
194485	Isoeruboside B	HDAC1	-7.2	Q13547	4BKX	Inhibitor
129394	4,7-Dihydroxy-5-methoxyl-6-methyl-8-formyl-flavan	GSTP1	-7.1	P09211	5J41	Inhibitor
194485	Isoeruboside B	HSP90AA1	-7.1	P07900	5J80	Inhibitor
5742590	Sitogluside	HSP90AA1	-7.1	P07900	5J80	Inhibitor
11658052	Simiglaside B	NFKB1	-7.1	P19838	2O61	Inhibitor
11764506	Simiglaside E	STAT1	-7.1	P42224	3WWT	Inhibitor
5280794	Stigmasterol	NFKB1	-7	P19838	2O61	Inhibitor
23666345	Sodium taurocholate	STAT3	-7	P40763	6NJS	Inhibitor
5742590	Sitogluside	NFKB1	-6.8	P19838	2O61	Inhibitor
23666345	Sodium taurocholate	NFKB1	-6.8	P19838	2O61	Inhibitor
23666345	Sodium taurocholate	LMNA	-6.7	P02545	1IFR	Activator
11972467	Simiglaside C	SERPINE1	-6.6	P05121	7AQF	Inhibitor
102369777	Simiglaside D	SERPINE1	-6.6	P05121	7AQF	Inhibitor
11658052	Simiglaside B	SERPINE1	-6.5	P05121	7AQF	Inhibitor
128735	Isobaimuxinol	HSP90AA1	-6.4	P07900	5J80	Inhibitor
128735	Isobaimuxinol	CTSB	-6.2	P07858	6AY2	Inhibitor
194485	Isoeruboside B	HIF1A	-6.2	Q16665	4H6J	Inhibitor
102369777	Simiglaside D	NFKB1	-6.2	P19838	2O61	Inhibitor
129394	4,7-Dihydroxy-5-methoxyl-6-methyl-8-formyl-flavan	SERPINE1	-6.2	P05121	7AQF	Inhibitor
11658052	Simiglaside B	STAT1	-6.2	P42224	3WWT	Inhibitor
129394	4,7-Dihydroxy-5-methoxyl-6-methyl-8-formyl-flavan	NFKB1	-6.1	P19838	2O61	Inhibitor
11764506	Simiglaside E	SERPINE1	-6.1	P05121	7AQF	Inhibitor
11764506	Simiglaside E	NFKB1	-6	P19838	2O61	Inhibitor
222284	beta-sitosterol	CTSB	-5.9	P07858	6AY2	Inhibitor
102369777	Simiglaside D	STAT1	-5.8	P42224	3WWT	Inhibitor
222284	beta-sitosterol	STAT3	-5.8	P40763	6NJS	Inhibitor
128735	Isobaimuxinol	CTSK	-5.7	P43235	4X6H	Inhibitor
128735	Isobaimuxinol	STAT3	-5.7	P40763	6NJS	Inhibitor
11972467	Simiglaside C	NFKB1	-5.6	P19838	2O61	Inhibitor
128735	Isobaimuxinol	NFKB1	-5.5	P19838	2O61	Inhibitor
129394	4,7-Dihydroxy-5-methoxyl-6-methyl-8-formyl-flavan	HIF1A	-5.3	Q16665	4H6J	Inhibitor
11764506	Simiglaside E	HIF1A	-5.3	Q16665	4H6J	Inhibitor
222284	beta-sitosterol	NFKB1	-5.3	P19838	2O61	Inhibitor
11972467	Simiglaside C	STAT1	-5.3	P42224	3WWT	Inhibitor
11658052	Simiglaside B	HIF1A	-4.8	Q16665	4H6J	Inhibitor
102369777	Simiglaside D	HIF1A	-4.8	Q16665	4H6J	Inhibitor
11972467	Simiglaside C	HIF1A	-4.7	Q16665	4H6J	Inhibitor

Inhibitors and activators are summarized based on the binding sites of the original ligands of proteins and their functions, which are of reference value.

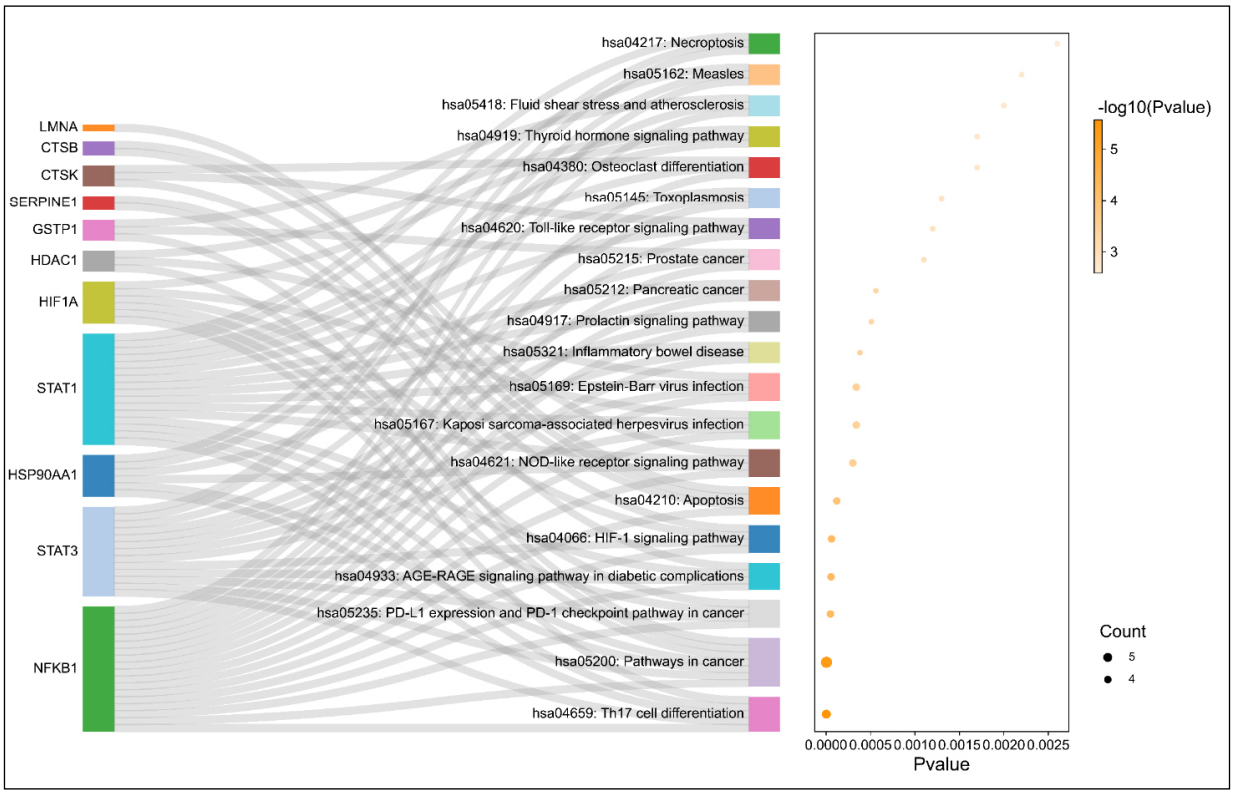

Figure 6. KEGG analysis of the screened 11 targets.

resorption in osteoporotic patients and to eliminate the sequelae of long-term BPs treatment.

Our studies show that CTSK can stably inhibit osteoclast differentiation and regulate signaling pathways such as toll-like receptor and apotosis. It is noteworthy that the active components of SGR, stigmasterol and beta-sitosterol, bind well with CTSK protein. Based on the original ligands of CTSK, we know that the binding of stigmasterol and beta-sitosterol to CTSK is reversed. That is, stigmasterol and beta-sitosterol can inhibit CTSK activity to inhibit osteoclast differentiation, thereby blocking bone resorption, demonstrating their potential for the treatment of osteoporosis.

In humans, the transcription factor nuclear factor kappa B subunit 1 (NFKB1) is a key regulator of many cellular processes including cell survival and inflammation. It participates in the body's inflammatory response, immune response, can regulate apoptosis, stress response, and over-activation of nuclear factor kappa B (NF-κB), which is associated with many human diseases such as rheumatoid arthritis[23], heart[24] and brain diseas[25]. Therefore, drugs can inhibit the NF-κB signaling pathway. It may become an important means for treating such diseases. The full name of RANKL is receptor activator of nuclear factor- kappa B ligand, which plays an important role in bone metabolism, regulates bone regeneration and remodeling[26]. In order to investigate the relationship between RANKL and NFKB1, researchers knocked out NFKB1 to investigate the effects of mechanical unloading (in microgravity or during bed rest) on bone loss[27].

The results show that NFKB1 deficiency inhibits mechanical unload-induced osteogenesis by maintaining the proportion and/or potential of osteoprogenic or immature osteoblasts and inhibiting bone resorption by inhibiting intracellular signals of RANKL, the precursor of osteoclasts. Our results show that there are several components in SGR that inhibit NFKB1, such as diosgenin, smilagenin, isoeruboside B, and similaside B. These components of SGR not only bind well to NFKB1, and in the molecular dynamics simulation examples given by us, the

stability of the systems of diosgenin and NFKB1 is good, which means that the simulation systems of other components and NFKB1 also perform well, that is, the components of SGR have a significant inhibitory effect on NFKB1.

It is worth mentioning that the hierarchy set up in this paper provides reference and guidance for future research. In recent years, in the field of molecular docking, it is common to study the binding of a single compound to a target protein. Although several compounds sometimes bind to the same protein, there is no additional binding energy. Therefore, in future studies we should focus on the computational procedures and binding effects of molecular docking. Similarly, in molecular dynamics simulation, although describing the movement of a compound and a protein in the same system, this does not clearly show the interaction of the compound with other proteins (which is unavoidable in the real environment), so these issues will be taken into account in future studies.

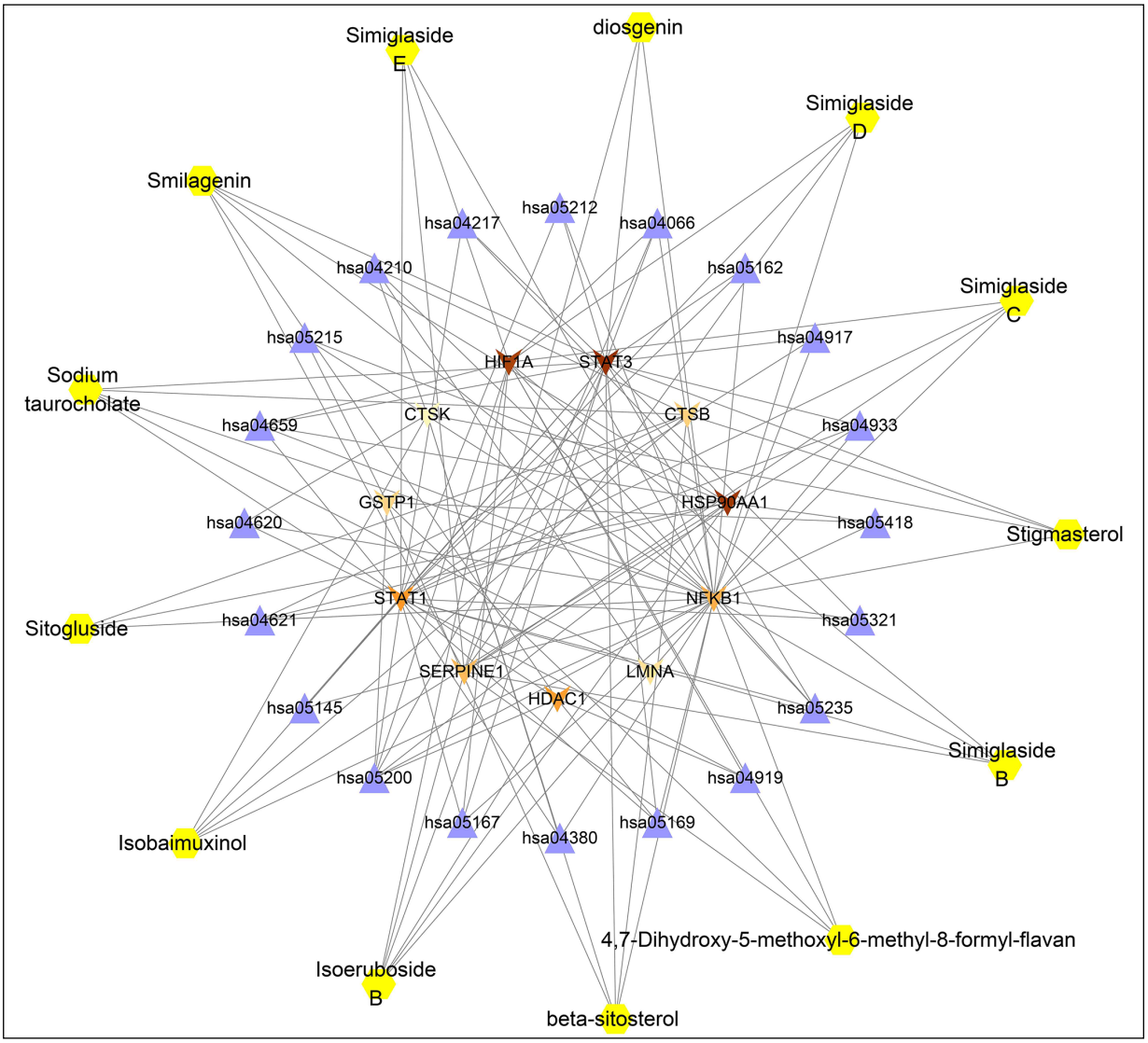

Figure 7. Components of SGR and C-T-P network of osteoporosis targets.

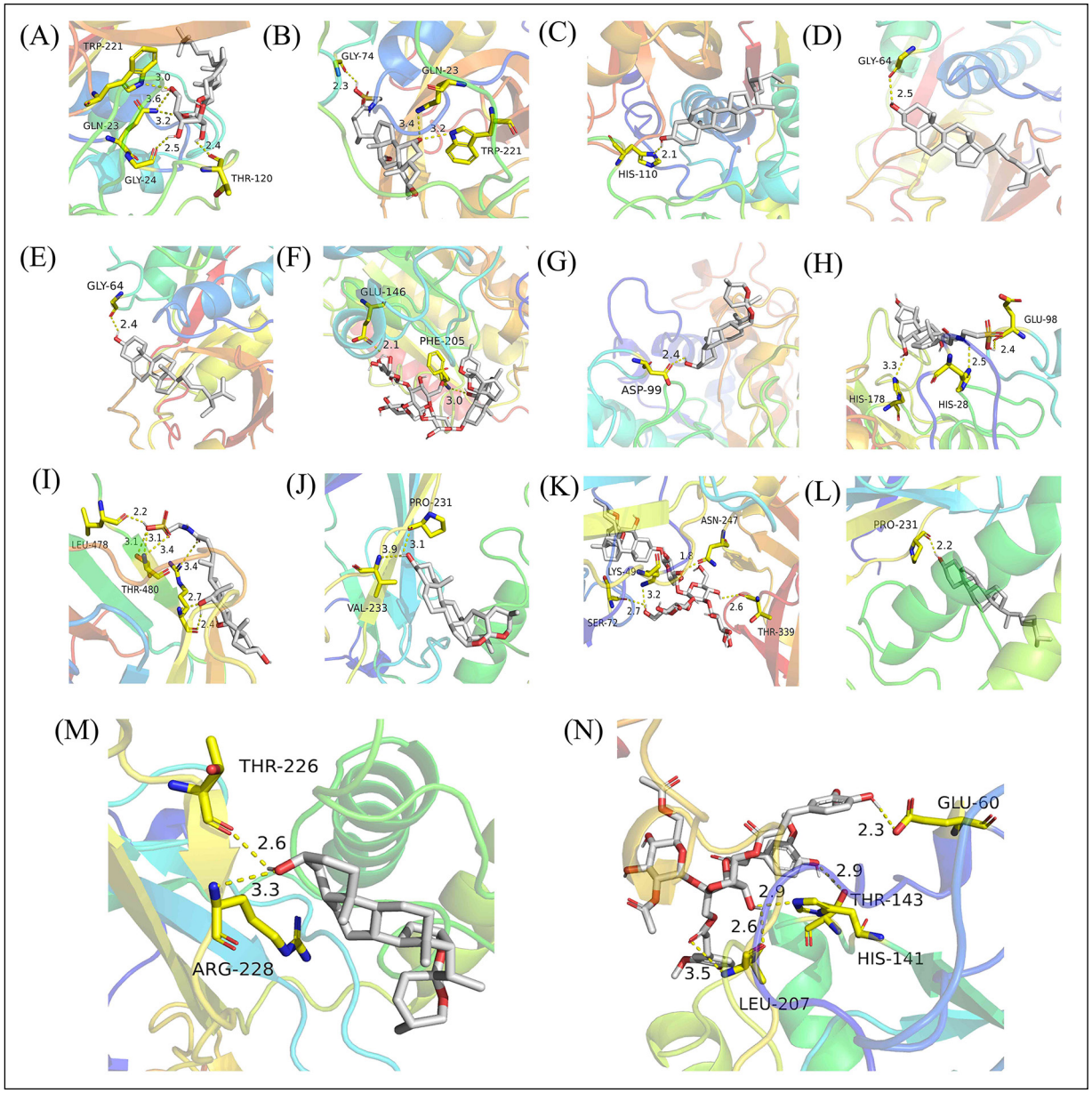

Figure 8. Molecular docking results of 6 components of SGR and 5 proteins of osteoporosis, the connection represents a hydrogen bond (**A**) *CTSB*-Sitogluside, (**B**) *CTSB*-Sodium taurocholate, (**C**) *CTSB*-Stigmasterol, (**D**) *CTSK*-beta-sitosterol, (**E**) *CTSK*-Stigmasterol, (**F**) *HDAC1*-Isoeruboside B, (**G**) *HDAC1*-Smilagenin, (**H**) *HDAC1*-Sodium taurocholate, (**I**) *LMNA*-Sodium taurocholate, (**J**) *NFKB1*-diosgenin, (**K**) *NFKB1*-Isoeruboside B, (**L**) *NFKB1*-Stigmasterol, (**M**) *NFKB1*-Smilagenin, (**N**) *NFKB1*-Simiglaside B. The yellow dotted line indicates the hydrogen bond, and the number indicates the bond length.

Conclusions

Our studies show that SGR can inhibit CTSK activity to inhibit osteoclast differentiation, thereby blocking bone resorption. Furthermore, there are several components in SGR that inhibit NFKB1. NFKB1 deficiency inhibits mechanical unload-induced osteogenesis by inhibiting bone resorption by inhibiting intracellular signals of RANKL, the precursor of osteoclasts. In summary, our study successfully explains the effective

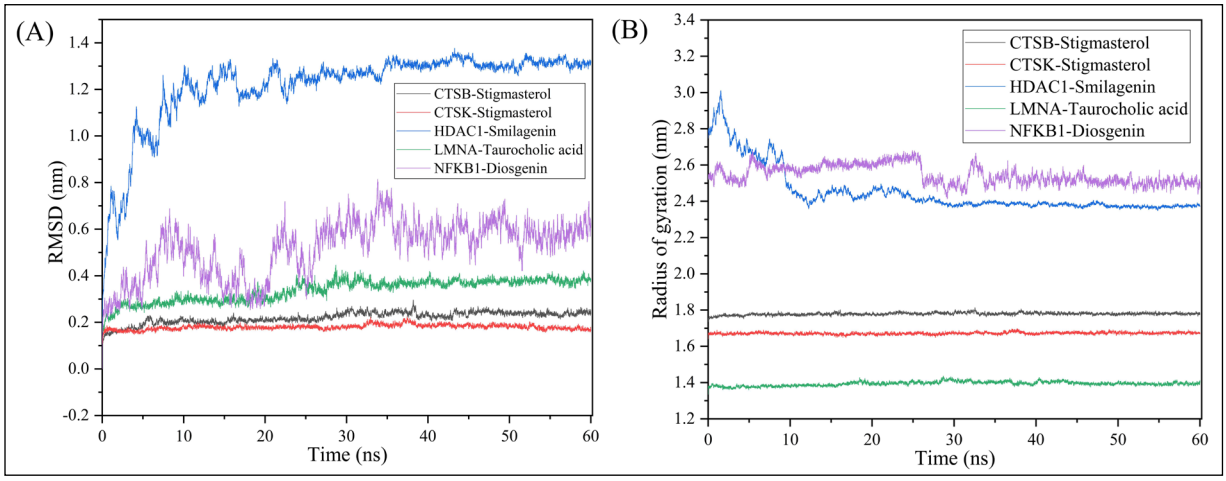

Figure 9. Display of MD simulation results. **A**, Root mean square deviation (RMSD). **B**, Radius of gyration (total and around axes).

mechanism by which SGR ameliorates osteoporosis while predicting the potential targets NFKB1 and CTSK of SGR for the treatment of osteoporosis.

Conflict of Interest

The Authors declare that they have no conflict of interests.

Availability of Data and Materials

Publicly available datasets were analyzed in this study. The Traditional Chinese Medicine Systems Pharmacology Database and Analysis Platform can be found at the following URL: https://tcmsp-e.com/tcmsp.php. The DrugBank database can be found at the following URL: https://www.drugbank.com/. The DisGeNET database can be found at the following URL: https://www.disgenet.org/. The Genecards database can be found at the following URL: https://www.genecards.org/. The GEO database can be found at the following URL: https://www.ncbi.nlm.nih.gov/geo/.

Ethics Approval

Not applicable.

Informed Consent

Not applicable.

ORCID ID

G. Li: 0000-0002-4587-6650.

Acknowledgements

We would like to acknowledge the following financial support: the National Natural Science Foundation of China (No. 82205154 and No. 82074453); the National Natural Science Foundation of Shandong Province (No. ZR2021QH004 and No. ZR2021LZY002); the Development Plan of Shandong Medical and Health Technology (No. 2019WS577 and No. 202104070600); the Development Plan of Shandong Traditional Chinese Medicine Science and Technology (No. 2020Q009 and No. 2020Q130); and the Innovation Program of Jinan Clinical Medicine Science and Technology (No. 202019056). We thank the NCBI GEO database for sharing the data.

Funding

This work was supported by grants from the National Natural Science Foundation of China (No. 82205154 and No. 82074453); the National Natural Science Foundation of Shandong Province (No. ZR2021QH004 and No. ZR2021LZY002); the Development Plan of Shandong Medical and Health Technology (No. 2019WS577 and No. 202104070600); the Development Plan of Shandong Traditional Chinese Medicine Science and Technology (No. 2020Q009 and No. 2020Q130); and the Innovation Program of Jinan Clinical Medicine Science and Technology (No. 202019056).

Authors' Contributions

All authors made a significant contribution to the work reported and agreed to be accountable for all aspects of the work. L.G. and L.B.W designed the experiments. L.B.W., L.X.Z., W.M.T., and L.G performed the experiments. L.B.W. and L.X.Z. prepared the initial draft of the manuscript. L.G. gave critical feedback during the study or during the submission of the manuscript. All authors provided final approval of the version to be submitted and agreed on the journal for publication.

References

1) Li SS, He SH, Xie PY, Li W, Zhang XX, Li TF, Li DF. Recent Progresses in the Treatment of Osteoporosis. Front Pharmacol 2021; 12: 717065.
2) Zeng Q, Li N, Wang Q, Feng J, Sun D, Zhang Q, Huang J, Wen Q, Hu R, Wang L, Ma Y, Fu X, Dong S, Cheng X. The Prevalence of Osteoporosis in China, a Nationwide, Multicenter DXA Survey. J Bone Miner Res 2019; 34: 1789-1797.
3) Si L, Winzenberg TM, Jiang Q, Chen M, Palmer AJ. Projection of osteoporosis-related fractures and costs in China: 2010-2050. Osteoporos Int 2015; 26: 1929-1937.
4) Ru J, Li P, Wang J, Zhou W, Li B, Huang C, Li P, Guo Z, Tao W, Yang Y, Xu X, Li Y, Wang Y, Yang L. TCMSP: a database of systems pharmacology for drug discovery from herbal medicines. J Cheminform 2014; 6: 13.
5) Zhang D, Wang Z, Li J, Zhu J. Exploring the possible molecular targeting mechanism of Saussurea involucrata in the treatment of COVID-19 based on bioinformatics and network pharmacology. Comput Biol Med 2022; 146: 105549.
6) Wishart DS, Knox C, Guo AC, Cheng D, Shrivastava S, Tzur D, Gautam B, Hassanali M. DrugBank: a knowledgebase for drugs, drug actions and drug targets. Nucleic Acids Res 2008; 36: D901-D906.
7) Bauer-Mehren A, Rautschka M, Sanz F, Furlong LI. DisGeNET: a Cytoscape plugin to visualize, integrate, search and analyze gene-disease networks. Bioinformatics 2010; 26: 2924-2926.
8) Shannon P, Markiel A, Ozier O, Baliga NS, Wang JT, Ramage D, Amin N, Schwikowski B, Ideker T. Cytoscape: a software environment for integrated models of biomolecular interaction networks. Genome Res 2003; 13: 2498-2504.
9) Huang da W, Sherman BT, Lempicki RA. Systematic and integrative analysis of large gene lists using DAVID bioinformatics resources. Nat Protoc 2009; 4: 44-57.
10) Xiong G, Wu Z, Yi J, Fu L, Yang Z, Hsieh C, Yin M, Zeng X, Wu C, Lu A, Chen X, Hou T, Cao D. ADMETlab 2.0: an integrated online platform for accurate and comprehensive predictions of ADMET properties. Nucleic Acids Res 2021; 49: W5-W14.
11) Morris GM, Goodsell DS, Huey R, Olson AJ. Distributed automated docking of flexible ligands to proteins: parallel applications of AutoDock 2.4. J Comput Aided Mol Des 1996; 10: 293-304.
12) Trott O, Olson AJ. AutoDock Vina: improving the speed and accuracy of docking with a new scoring function, efficient optimization, and multithreading. J Comput Chem 2010; 31: 455-461.
13) Seeliger D, de Groot BL. Ligand docking and binding site analysis with PyMOL and Autodock/Vina. J Comput Aided Mol Des 2010; 24: 417-422.
14) [14] Rakhshani H, Dehghanian E, Rahati A. Enhanced GROMACS: toward a better numerical simulation framework. J Mol Model 2019; 25: 355.
15) Tando T, Sato Y, Miyamoto K, Morita M, Kobayashi T, Funayama A, Kanaji A, Hao W, Watanabe R, Oike T, Nakamura M, Matsumoto M, Toyama Y, Miyamoto T. Hif1α is required for osteoclast activation and bone loss in male osteoporosis. Biochem Biophys Res Commun 2016; 470: 391-396.
16) Miyauchi Y, Sato Y, Kobayashi T, Yoshida S, Mori T, Kanagawa H, Katsuyama E, Fujie A, Hao W, Miyamoto K, Tando T, Morioka H, Matsumoto M, Chambon P, Johnson RS, Kato S, Toyama Y, Miyamoto T. HIF1α is required for osteoclast activation by estrogen deficiency in postmenopausal osteoporosis. Proc Natl Acad Sci U S A 2013; 110: 16568-16573.
17) Cousins KR. Computer review of ChemDraw Ultra 12.0. J Am Chem Soc 2011; 133: 8388.
18) Berman HM, Westbrook J, Feng Z, Gilliland G, Bhat TN, Weissig H, Shindyalov IN, Bourne PE. The Protein Data Bank. Nucleic Acids Res 2000; 28: 235-242.
19) Aminoshariae A, Donaldson M, Horan M, Mackey SA, Kulild JC, Baur D. Emerging antiresorptive medications and their potential implications for dental surgeries. J Am Dent Assoc 2022; 153: 649-658.
20) Matuszewska A, Matuszewski Ł, Jaszek M, Polak P, Stec S. Effect of bisphosphonates on selected markers of bone turnover in patients after total knee arthroplasty. Int Orthop 2022; 46: 1529-1538.
21) Gao LH, Li SS, Yue H, Zhang ZL. Associations of Serum Cathepsin K and Polymorphisms in CTSK Gene With Bone Mineral Density and Bone Metabolism Markers in Postmenopausal Chinese Women. Front Endocrinol (Lausanne) 2020; 11: 48.
22) Zajic S, Stoch SA, McCrea JB, Witter R, Fayad GN, Martinho M, Stone JA. A phase 1 pooled PK/PD analysis of bone resorption biomarkers for odanacatib, a Cathepsin K inhibitor. J Pharmacokinet Pharmacodyn 2020; 47: 473-484.
23) Lee WS, Kato M, Sugawara E, Kono M, Kudo Y, Kono M, Fujieda Y, Bohgaki T, Amengual O, Oku K, Yasuda S, Onodera T, Iwasaki N, Atsumi T. Protective Role of Optineurin Against Joint Destruction in Rheumatoid Arthritis Synovial Fibroblasts. Arthritis Rheumatol 2020; 72: 1493-1504.
24) Wang Y, Wu B, Zhang M, Miao H, Sun J. Significant association between rs28362491 polymorphism in NF-κB1 gene and coronary artery disease: a meta-analysis. BMC Cardiovasc Disord 2020; 20: 278.
25) Long J, Tian L, Baranova A, Cao H, Yao Y, Rao S, Zhang F. Convergent lines of evidence supporting involvement of NFKB1 in schizophrenia. Psychiatry Res 2022; 312: 114588.
26) Tang CY, Wang H, Zhang Y, Wang Z, Zhu G, McVicar A, Li YP, Chen W. GPR125 positively regulates osteoclastogenesis potentially through AKT-NF-κB and MAPK signaling pathways. Int J Biol Sci. 2022; 18: 2392-2405.
27) Nakamura H, Aoki K, Masuda W, Alles N, Nagano K, Fukushima H, Osawa K, Yasuda H, Nakamura I, Mikuni-Takagaki Y, Ohya K, Maki K, Jimi E. Disruption of NF-κB1 prevents bone loss caused by mechanical unloading. J Bone Miner Res 2013; 28: 1457-1467.